

Spatial disease mapping using Directed Acyclic Graph Auto-Regressive (DAGAR) models

BY A. DATTA

Department of Biostatistics, Johns Hopkins University, Baltimore, Maryland 21205, USA
abhidatta@jhu.edu

S. BANERJEE

Department of Biostatistics, University of California, Los Angeles, California 90095, USA
sudipto@ucla.edu

J. S. HODGES

Division of Biostatistics, University of Minnesota, Twin Cities, Minnesota 55455, USA
hodge003@umn.edu

SUMMARY

Hierarchical models for regionally aggregated disease incidence data commonly involve region specific latent random effects that are modelled jointly as having a multivariate Gaussian distribution. The covariance or precision matrix incorporates the spatial dependence between the regions. Common choices for the precision matrix include the widely used intrinsic conditional autoregressive model, which is singular, and its nonsingular extension which lacks interpretability. We propose a new parametric model for the precision matrix based on a directed acyclic graph representation of the spatial dependence. Our model guarantees positive definiteness and, hence, in addition to being a valid prior for regional spatially correlated random effects, can also directly model the outcome from dependent data like images and networks. Theoretical and empirical results demonstrate the interpretability of parameters in our model. Our precision matrix is sparse and the model is highly scalable for large datasets. We also derive a novel order-free version which remedies the dependence of directed acyclic graphs on the ordering of the regions by averaging over all possible orderings. The resulting precision matrix is available in closed form. We demonstrate the superior performance of our models over competing models using simulation experiments and a public health application.

Some key words: Bayesian inference; Directed acyclic graph; Disease mapping; Spatial autoregression

1. INTRODUCTION

Epidemiological data for disease rates are often presented as aggregated disease counts over entire geographical regions like states or counties. Such *areal* or *areally-referenced* data are ubiquitous in public health applications. Accurate identification of trends and factors associated with the disease requires accounting for the spatial dependence among the regions. A common approach to analyse areal datasets envisions the geographic domain as an undirected graph with the regions constituting the vertices and an edge between two vertices if the corresponding regions share a geographical border. This creates well defined neighbours for each region which

are used to specify the joint or conditional distributions of region-specific latent Gaussian random effects in a hierarchical setup. For example, the popular conditional autoregressive model (Besag, 1974; Clayton & Bernardinelli, 1992) incorporates the underlying neighbourhood structure in specifying the full conditional distribution for each observation. If w_i denotes the random effect representing the i th region for $i = 1, \dots, k$ and $i \sim j$ indicates that regions i and j are neighbours, then the conditional autoregressive model specifies the full conditional distributions

$$w_i | w_{-i} \sim N \left(\sum_{j \sim i} w_j / n_i, \tau_w n_i \right), \quad (1)$$

where w_{-i} denotes the vector of observations leaving out the i th one, n_i denotes the number of neighbours for the i th region and throughout the text we adopt the convention that $N(\alpha, \Delta)$ denotes normal distribution with mean α and precision Δ , both in univariate and multivariate contexts. Hence, in (1) above, $\tau_w n_i$ is the conditional precision of $w_i | w_{-i}$.

The joint distribution of $w = (w_1, \dots, w_k)^T$ can be derived from (1) as $w \sim N(0, \tau_w(D - A))$ where $A = (a_{ij})$ is the adjacency matrix of the neighbourhood graph i.e. $a_{ij} = 1$ if and only if $i \sim j$, and D is a diagonal matrix with n_1, \dots, n_k on the diagonal. As $D - A$ is singular, this construction yields an improper joint distribution of the w_i 's, referred to as the intrinsic or improper conditional autoregressive model. This impropriety renders the model ineligible for directly modelling the response or for generating data, although both can proceed by using contrasts as demonstrated in Besag & Kooperberg (1995). Also, the distribution can still be used as a prior for latent spatial random effects w and the posterior of w usually remains valid.

The impropriety of the intrinsic conditional autoregressive model can be rectified by generalising the full conditional mean to $E(w_i | w_{-i}) = \rho \sum_{j \sim i} w_j / n_i$ yielding the joint distribution $w \sim N(0, \tau_w(D - \rho A))$ which is proper for a certain range of ρ . Although introduction of ρ imparts more flexibility than the parameter-free improper analogue, it is difficult to interpret ρ as even very high values of ρ induce only modest spatial correlation among the observations (see Banerjee et al., 2014, for a discussion on this). Furthermore, Wall (2004) shows that even negative values of ρ may lead to positive correlation among neighbouring regions. Assuncao & Krainski (2009) found that these oddities are a general feature of conditional autoregressive models.

The second popular approach is the simultaneous autoregressive model (Whittle, 1954) which proceeds by simultaneously modelling the random effects as

$$w_i = \sum_{j \neq i} b_{ij} w_j + \epsilon_i \text{ for } i = 1, 2, \dots, k \quad (2)$$

where $\epsilon_i \stackrel{\text{ind}}{\sim} N(0, \tau_i)$ are errors independent of w . Defining $B = (b_{ij})$ and F to be a diagonal matrix with entries τ_1, \dots, τ_k , the set of equations in (2) yields the joint distribution $w \sim N(0, (I - B)F(I - B)^T)$. However, the common choice of defining $b_{ij} = \rho I(i \sim j) / n_i$, where $I(\cdot)$ denotes the indicator function, leads to similar problems with respect to interpretation of the parameter ρ (Wall, 2004).

Beyond these two approaches, the inventory of covariance models for areal datasets is very limited. Leroux et al. (2000) and MacNab & Dean (2000) extended the conditional autoregressive model by accommodating over-dispersion alongside spatial information. They proposed using the precision matrix $\lambda \tau_w(D - A) + (1 - \lambda) \tau_w I$, where $\lambda \in [0, 1]$ controls the degree of dependence among the regions. For a regular graph where all vertices have same number of neighbours d , $D = dI$. In this case, $\lambda \tau_w(D - A) + (1 - \lambda) \tau_w I$ can be rewritten as $\frac{1+(d-1)\lambda}{d} \tau_w(D - \rho^* A)$

where $\rho^* = \frac{d\lambda}{1+(d-1)\lambda}$. Thus, if the numbers of neighbours for the vertices do not vary greatly, this approach is somewhat similar to the proper conditional autoregressive model and is encumbered by the same interpretability concerns. Also, this model requires computationally expensive determinant calculations for large datasets.

For lattice based applications, there is a richer class of parametric intrinsic autoregression models (Besag & Kooperberg, 1995; Besag & Higdon, 1999). Likelihoods of these models can also be evaluated expediently using the scalable algorithm developed in Dutta & Mondal (2015). However, all such intrinsic models rely heavily on the lattice structure and cannot be used directly for arbitrary graphs. Applications to irregular areal data can proceed by breaking up the region into a fine lattice, using the intrinsic model on the lattice and aggregating over each area. Besag & Mondal (2005) demonstrated that for certain classes of intrinsic autoregressive models, the aggregated model is asymptotically equivalent to aggregating an anisotropic de Wijs Gaussian Process over the entire domain. These results impart interpretability to the parameters of the intrinsic autoregression. In certain applications, e.g., in agricultural experiments, one can readily envision an underlying spatial process representing the fertility of the soil at a fine scale. This is, however, less clear in disease mapping contexts where the data are often observed over fixed politically delineated regions and such a latent fine scale spatial process may not have any interpretation. In this manuscript, we only focus on models that can be formulated directly on the areal units.

This manuscript proposes a new way of constructing precision matrices for areal models using a directed acyclic graph derived from the original undirected graph. Directed acyclic graphs or DAGs have been used in the spatial literature for modelling large spatial datasets (Datta et al., 2016a) and for generating image textures (Cressie & Davidson, 1998). Instead of modelling the precision matrix directly, we model its Cholesky factor, which for any multivariate Gaussian distribution is determined by the conditional distributions of the w_i 's. We specify these conditional distributions using autoregressive covariance models on a sequence of local trees created from this directed acyclic graph. The resulting Cholesky factor and the precision matrix are sparse. We refer to this model as the directed acyclic graph autoregressive or DAGAR model.

Unlike the improper conditional autoregressive model, our model's covariance matrix is guaranteed to be positive definite. This opens up a new avenue to generate or directly model multivariate Gaussian data with dependence structure derived from a graph. Common examples of such data, besides aggregated regional data, include images or social network data. We establish, both theoretically and empirically, that our model endows ρ with a clear interpretation as a spatial autocorrelation parameter, which, in fact, resolves an important conundrum in the conditional and simultaneous autoregressive models (Wall, 2004). Also, the Cholesky factor has the same level of sparsity as the undirected graph ensuring scalability for analysing very large areal datasets.

Cholesky factors inherit the dependence of directed acyclic graphs on ordering of the regions, thereby making our model order-dependent. As spatial regions generally do not have any natural ordering, we also propose a novel order free model by averaging over all $k!$ possible orderings. We show that the resulting precision matrix, which is order-free, can be evaluated in closed form. We present some theoretical results that suggest the DAGAR precision matrix with a reasonably chosen ordering is often similar to the order-free matrix. Simulation experiments also show that the order-dependent and order-free models produce extremely similar results and, for most scenarios, both outperform conditional autoregressive models in their ability to correctly estimate a latent spatial surface.

2. METHOD

2.1. Modelling Cholesky Factors

We first review a general approach to modelling Gaussian covariance matrices using sparse Cholesky factors and discuss how this relates to conditional autoregressive models and general covariance estimation. This will help to motivate the subsequent construction of our model in Section 2.2. We assume that the graph of the regions is connected. Disconnected graphs with multiple islands will entail a simple extension with block diagonal covariance structures, where each block represents an island. Let $\mathcal{G} = (V, E)$ denote the connected graph with the regions as vertices V and edges E between neighbours. We denote the i th region simply by i and let $A = (a_{ij})$ denote the adjacency matrix for this undirected graph. To model Cholesky factors we specify distributions of the w_i 's as

$$w_1 = \epsilon_1, w_2 = b_{21}w_1 + \epsilon_2, \dots, w_k = b_{k1}w_1 + \dots + b_{k,k-1}w_{k-1} + \epsilon_k, \quad (3)$$

where the ϵ_i 's are independent $N(0, \tau_i)$ errors. $B = (b_{ij})$ is now a strictly lower triangular matrix. Let F be the diagonal matrix with τ_1, \dots, τ_k on the diagonal. Then $w \sim N(0, L^T FL)$ where $L = I - B$. Switching from the specification in (2) to a strictly lower triangular matrix B is not restrictive because of the following result.

THEOREM 1. *Let $w \sim N(0, Q)$ where Q is the (possibly singular) precision matrix. Then there exists a permutation matrix P , a strictly lower triangular matrix B and a diagonal matrix F with non-negative entries such that $PQP^\top = (I - B)^\top F(I - B)$.*

While this result is trivial if Q is non-singular, for rank deficient Q this relies on the algorithm for obtaining the Cholesky factor. All proofs are presented in Section A of the Appendix. Hence, any multivariate normal distribution can be expressed as in (3) under certain orderings of the areal units. For low rank distributions this will be equivalent to setting some of the τ_i 's to zero. In fact, switching to the lower triangular B has several advantages. First, L is lower triangular with ones on the diagonal, guaranteeing that $L^T FL$ is positive definite as long as all τ_i 's are positive. Also $\det(L^T FL)$ is simply $\prod_{i=1}^n \tau_i$ and the quadratic form $w^T L^T FL w$ can be expressed as $\tau_1 w_1^2 + \sum_{i=2}^k \tau_i (w_i - \sum_{\{j < i\}} w_j b_{ij})^2$, evaluating which requires $\mathcal{O}(k + s)$ floating point operations (FLOPs) where s is the sparsity, i.e., the number of non-zero entries of B . Hence, if B is sparse, the joint density of w can be evaluated in an extremely scalable manner.

To complete the specification in (3), we need to fully specify the matrices B and F . The parameters $\{b_{ij}\}$ and $\{\tau_i\}$ are identifiable up to a marginal precision parameter because the factorisation $(I - B)^\top F(I - B)$ is the LDL^T factorisation (a variant of Cholesky decomposition with ones on the diagonal of L), which is unique. If multiple datapoints exist for each region, we can estimate B and F without imposing simplifying assumptions. In fact, since a sparse representation of the Cholesky factor $I - B$ is desired, the problem reduces to high-dimensional covariance or precision matrix estimation for which there exists a vast inventory of statistical methods including banding (Wu & Pourahmadi, 2003; Bickel & Levina, 2008b), tapering (Cai et al., 2010), thresholding (Bickel & Levina, 2008a; El Karoui, 2008; Rothman et al., 2009) and penalisation (Meinshausen & Bühlmann, 2006; Friedman et al., 2007; Xue et al., 2012) among others. On the other hand, for large point-referenced spatial datasets, Datta et al. (2016a,b), Finley et al. (2017) construct sparse Cholesky factor approximations of the precision matrix from a Matérn covariance function (Stein, 1999). These approximations are hence derived from an original joint distribution of the spatial random effects.

However, most areal datasets lack replication that would permit use of fully data-driven learning methods to estimate B and F . Also, unlike well defined Matérn Gaussian processes on con-

tinuous domains, there is no well defined covariance matrix on arbitrary graphs from which one can derive sparse Cholesky factors. In fact, our goal here is the opposite, that is to construct a multivariate Gaussian distribution on graphs starting from the sparse Cholesky factor. Consequently, we cannot estimate B and F in their most general form and need to make simplifying assumptions.

2.2. Directed acyclic graph autoregressive models

To achieve sparsity, we adopt the strategy of defining neighbour sets $N(i)$ such that $b_{ij} = 0$ for all $j \notin N(i)$. The choice and size of the neighbour sets for areal datasets can be predicated upon the underlying neighbourhood graph \mathcal{G} . For $i > 1$, we define $N(i) = \{j < i, j \sim i\}$. The constraint $j < i$ is necessary to endow B with a lower triangular structure. This reduces (3) to

$$w_1 = \epsilon_1, \quad w_i = \sum_{j \in N(i)} w_j b_{ij} + \epsilon_i, \quad (i = 2, \dots, k) \quad (4)$$

This specification is analogous to auto-regressive models for time series. In fact, if w_i denotes the response at time i , $N(i)$ includes all time points less than i up to a lag of r , and $b_{ij} = b_{i-j}$, then (4) simply denotes the autoregressive model of order r . In a time-series context, where i and j denote time points, assigning the weights b_{ij} based on the temporal lag seems natural, but for irregular areal datasets, enumeration of the areal units does not have any physical interpretation. Also in the context of image texture analysis, Cressie & Davidson (1998) used different coefficients for w_j in (4) based on the direction of neighbours on a regular lattice, to generate images with a wide range of textures. In general, vertices of irregular graphs based on areal datasets do not share such commonality in terms of spatial orientation of their neighbours. Hence, it is intuitive to assign equal weights to all the neighbours, i.e., letting $b_{ij} = b_i$ for all $j \in N(i)$. A natural choice would be to let $b_i = 1/n_{<i}$ and $\tau_i \propto n_{<i}$ where $n_{<i} = |N(i)|$ denotes the cardinality of the neighbour set. This specification is similar to (1) except that we are only using the directed neighbours $N(i)$ instead of all neighbours. Since $n_{<1} = 0$, this choice of b_{ij} leads to the conundrum of how to specify τ_1 . Either we need to define τ_1 in a manner inconsistent with the definition of τ_i for $i > 1$ or we define $\tau_1 = 0$ which yields an improper distribution for w . We circumvent this using a more general specification described below that includes the degenerate prior with $b_i = 1/n_{<i}$ and $\tau_i \propto n_{<i}$ as a limiting case.

Let d_{ij} denote the length of the shortest path on \mathcal{G} between nodes i and j . If \mathcal{G} is a tree, i.e., an acyclic graph, then for any $0 \leq \rho < 1$, the matrix with elements $\rho^{d_{ij}}$ is positive definite and can be used to model the covariance of w . This extends the AR(1) model for time series to any tree graph (Basseville et al., 2006). However, graphs corresponding to areal datasets are rarely acyclic and for loopy graphs such results generally do not hold. A spanning tree of a graph is a subgraph that is a tree and includes all the vertices of the original graph. Spanning trees have been used to iteratively approximate parametric covariance matrices over loopy graphs (Sudderth, 2002). Borrowing these ideas, a potential solution would be to define the covariance matrix for w as the AR(1) covariance matrix on a spanning tree of \mathcal{G} . However, for large graphs, strategies for deciding upon the best spanning tree are unclear and computationally expensive. Furthermore, as demonstrated in (Sudderth, 2002), ignoring certain edges when pruning \mathcal{G} to a spanning tree can lead to large errors. Instead, we will use local spanning tree embeddings of small subgraphs of \mathcal{G} to construct the lower dimensional conditional densities specified in (4). This method does not ignore any edge and yet produces a computationally convenient precision matrix.

Let \mathcal{G}_i be the subgraph of \mathcal{G} comprising vertices $\{i\} \cup N(i)$ and the edges among them. We intend to construct the conditional density $w_i | w_{N(i)}$ using an embedded spanning tree \mathcal{T}_i of \mathcal{G}_i . The natural candidate for \mathcal{T}_i is the tree $(\{i\} \cup N(i), \{i \sim j | j \in N(i)\})$ as it contains all edges

between i and $N(i)$. We specify the conditional density $w_i | w_{N(i)}$ using the AR(1) model on \mathcal{T}_i with parameter ρ . To be precise, for any $0 \leq \rho < 1$ we define $E(w_i | w_{N(i)}) = v_i^T \Sigma_i^{-1} w_{N(i)}$ and $\text{var}(w_i | w_{N(i)}) = 1 - v_i^T \Sigma_i^{-1} v_i$, where v_i is the $n_{<i} \times 1$ vector of covariances between w_i and $w_{N(i)}$ and Σ_i is the $n_{<i} \times n_{<i}$ AR(1) covariance matrix of $w_{N(i)}$. Equating this with (4), we have

$$b_{ij} = \frac{\rho}{1 + (n_{<i} - 1)\rho^2} \quad (i = 2, \dots, k; j \in N(i)), \quad \tau_i = \frac{1 + (n_{<i} - 1)\rho^2}{1 - \rho^2} \quad (i = 1, \dots, k) \quad (5)$$

The specifications in (5) reveals some desirable intuitive features. First, as discussed earlier, $b_{ij} = b_i$ for all $j \in N(i)$, thereby assigning equal weights to all the directed neighbours. Also, the conditional precision τ_i for w_i increases with the number of directed neighbours. The formulation of \mathcal{T}_i also ensures that any edge between i and j is incorporated in the conditional specification of w_i or w_j depending on which comes later in the ordering. So, unlike approximating the entire graph with a spanning tree, the local spanning tree approach ensures that no edge of \mathcal{G} is ignored. Furthermore, for any $0 \leq \rho < 1$ all τ_i 's are positive thereby ensuring a proper probability distribution $w \sim N(0, L^T F L)$. The limiting case of $\rho = 1$ is equivalent to the improper prior with $b_i = 1/n_{<i}$ and $\tau_i \propto n_{<i}$, when using the parametrisation $\tau_i = 1 + (n_{<i} - 1)\rho^2$ and absorbing $1/(1 - \rho^2)$ into the marginal variance of w .

The constructions in (3) and (5) assume a specific ordering, which we now generalise to any other ordering. Let $\pi = \{\pi(1), \dots, \pi(n)\}$ be any predetermined ordering of the regions and π^{-1} denote its corresponding inverse permutation. Under this ordering, for any $i \neq \pi(1)$, we define its past observations as $w_{<i, \pi}$ as the collection $\{w_j | \pi^{-1}(j) < \pi^{-1}(i)\}$ and its set of directed neighbours $N_\pi(i) = \{j | i \sim j, \pi^{-1}(j) < \pi^{-1}(i)\}$. Let E_π denote the collection of directed edges from all members of $N_\pi(i)$ to i for every $i \neq \pi(1)$. We now have a directed acyclic graph $\mathcal{D}_\pi = (V, E_\pi)$. Let $n_{\pi(i)} = |N_\pi(i)|$. The generalisation of (5) based on \mathcal{D}_π is:

$$w_i | w_{<i, \pi} \sim N \left(\frac{\rho}{1 + (n_{\pi(i)} - 1)\rho^2} \sum_{j \in N_\pi(i)} w_j, \frac{1 + (n_{\pi(i)} - 1)\rho^2}{1 - \rho^2} \right), \quad (6)$$

where for any i that has no directed neighbours under π , $n_{\pi(i)} = 0$ and the conditional mean in (6) is zero. If $w_\pi = (w_{\pi(1)}, \dots, w_{\pi(k)})^T$, and L_π and F_π denote the analogous matrices corresponding to this ordering π , then we have

$$w_\pi \sim N(0, L_\pi^T F_\pi L_\pi) \quad (7)$$

This completes the specification of a new class of covariance models for areal datasets. Since the construction is predicated upon a directed acyclic graph derived from an original graph \mathcal{G} , we refer to this as the directed acyclic graph autoregressive or DAGAR model. Since L_π is lower triangular with $e = |E|$ non-zero sub-diagonal entries and F_π is diagonal, for any ρ , the determinant of $\text{cov}(w_\pi)$ is simply $(1 - \rho^2)^k / \prod_{i=1}^k (1 + (n_{\pi(i)} - 1)\rho^2)$ and the likelihood for the model in (7) can be evaluated using $\mathcal{O}(k + e)$ FLOPs. This ensures that our model is highly scalable and can be used to analyse massive areal datasets.

We also obtain insight about the interpretability of ρ from certain special graphs.

THEOREM 2. *Let \mathcal{T} denote a tree with vertices $V = \{1, \dots, k\}$ and π denote any ordering such that for any $i \neq \pi(1)$, $n_\pi(i) = 1$. Then the covariance matrix in (7) defines the autoregressive Gaussian process on \mathcal{T} , i.e., $(L_\pi^T F_\pi L_\pi)^{-1} = (\rho^{d_{ij}})$ where d_{ij} denotes the shortest path on \mathcal{T} between i and j .*

Theorem 2 shows that if \mathcal{G} is acyclic, then under certain orderings including breadth-first and pre-order tree traversals, this model is equivalent to the stationary AR(1) model on trees with

ρ being the correlation between neighbouring areas. In fact, in this case, for any two vertices separated by a distance d , the correlation is ρ^d . The result also shows that while we require an ordering of the locations to construct the DAGAR model, the resulting matrix can often be order-free and stationary and simply a function of the underlying undirected graph. We now present a result on interpretation of ρ for an $m \times n$ regular grid graph.

THEOREM 3. *Let \mathcal{G} denote the $m \times n$ grid graph with vertices $V = \{(i, j) \mid i = 1, \dots, m; j = 1, \dots, n\}$ and neighbours to the north, south, east, and west, and let π denote any ordering of the vertices corresponding to non-decreasing or non-increasing order of $i + j$ or $i - j$, then $\text{var}(w_{(i,j)}) = 1$ for all i and j , and for any neighbouring pair of vertices (i, j) and (i', j') , $\text{cov}(w_{(i,j)}, w_{(i',j')}) = \rho$.*

Hence, although for a grid, the DAGAR precision matrix is a function of the ordering, for all orderings of Theorem 3, the model yields unit variances and a correlation of ρ for all neighbour pairs. Hence, ρ is still interpretable. Of course, it is difficult to generalise these interpretability results for irregular graphs. Nevertheless, numerical exercises detailed in Section 3.1 show that, even for irregular graphs, ρ in our model is substantially more interpretable than its analogous parameter in the proper conditional autoregressive model.

2.3. Order-free model

Unlike covariance or precision matrices that remain invariant up to a permutation factor under different orderings of the multivariate vector, Cholesky factors depend on the ordering of the observations. Our model in (7) assumes a predetermined ordering π . One approach would be to use simple intuitive orderings based on the coordinates representing the nodes in some Euclidean embedding of \mathcal{G} . Similar strategies have been used in Cholesky factor based approaches in Datta et al. (2016a), Stein et al. (2004) and Vecchia (1988) who observed empirically that the joint distribution seemed to be less sensitive to ordering of the regions. An alternative approach would be to use a prior on the ordering π over the space of all orderings and cycle through models of different orderings in a Bayesian setup. However, for k nodes there are $k!$ possible orderings, and even for very small k , approaches akin to Bayesian model averaging (Hoeting et al., 1999) will fail to explore even a small fraction of all possible orderings. Instead, we propose an order-free model using a product-of-experts type construction (Hinton, 2002). Let P_π denote the permutation matrix corresponding to π i.e. $P_\pi(x_1, \dots, x_k)^T = (x_{\pi(1)}, \dots, x_{\pi(k)})^T$ for any k -dimensional vector x , and let Q denote the average of the precision matrices in (7) over all permutations π , i.e.,

$$Q = \frac{1}{k!} \sum_{\pi} P_\pi^T L_\pi^T F_\pi L_\pi P_\pi . \quad (8)$$

It is clear that Q is free of any ordering and is only a function of the undirected graph \mathcal{G} . Also, since it is the average of positive definite matrices, it is also positive definite. The following theorem derives the closed form expression for Q .

THEOREM 4. *Let $i \approx j$ mean that i and j share at least one common neighbour. There exist functions $f(\rho, r)$ and $g(\rho, r)$ for any positive integer r and $0 \leq \rho < 1$ such that*

$$Q_{ii} = 1 + \frac{n_i \rho^2}{2(1 - \rho^2)} + \frac{\rho^2}{1 - \rho^2} \sum_{j \sim i} f(\rho, n_j)$$

$$Q_{ij} = -\frac{\rho}{1 - \rho^2} I(i \sim j) + \frac{1}{1 - \rho^2} I(i \approx j) \sum_{k \sim N(i) \cap N(j)} g(\rho, n_k)$$

where $I(\cdot)$ denotes the indicator function. Explicit expressions for $f(\rho, r)$ and $g(\rho, r)$ are provided in the proof of Theorem 4 in Section A-4 of the Appendix. If $n_{\max} = \max(n_i)$ then, for any given ρ , $f(\rho, r)$ and $g(\rho, r)$ for $r = 1, \dots, n_{\max}$ can be calculated using $\mathcal{O}(n_{\max})$ FLOPs. Subsequently each non-zero entry of Q can be evaluated using $\mathcal{O}(n_{\max})$ additional FLOPs. From Theorem 4, it is clear that for $i \neq j$, $Q_{ij} \neq 0$ if and only if either $i \sim j$ or $i \approx j$. Hence, the sparsity of Q is e_2 where e_2 is the number of edges in the second order graph created from \mathcal{G} . The total computational cost for evaluating Q is $\mathcal{O}(e_2 n_{\max})$.

As $e_2 > e$, Q is less sparse than the precision matrices for the original DAGAR model in Section 2.2 or the conditional autoregressive models. Furthermore, Q does not have a closed form expression for the determinant, which may invoke expensive computations. In applications where the second-order graph is very dense, evaluating the likelihood for the order-free model will be slow. It is conceivable to envision such a scenario for social network applications where some nodes tend to be ‘hubs’ with lots of neighbours leading to very dense second order graphs. However, for disease mapping, regions typically have only a few geographically neighbouring regions. As $e_2 < kn_{\max}(n_{\max} + 1)/2$, the second order graph will be conveniently sparse in most such applications as n_{\max} will be typically very small relative to k . Hence, Q will still remain very sparse and we can leverage sparse determinant calculations to expedite the likelihood evaluations.

Numerical analyses detailed in Section 3 show that for a wide range of scenarios, performance of the DAGAR model and its order-free version were very similar. We now present some theoretical results that shed some light into this.

THEOREM 5. *Let $Q(\rho)$ be the DAGAR precision matrix for a path graph $(\{i_1, i_2, \dots, i_k\}, \{i_j \sim i_{j+1} : i \leq j < k\})$: using left-to-right or right-to-left ordering. Also let $Q_{OF}(\rho)$ denote the order free DAGAR model. Then*

$$\lim_{k \rightarrow \infty} \frac{\|Q(\rho) - Q_{OF}(\rho)\|_F}{\|Q_{OF}(\rho)\|_F} = \sqrt{\frac{4\rho^8 + 2\rho^4}{(3 + 6\rho^2 + \rho^4)^2 + 18\rho^2(1 + \rho^2)^2 + 2\rho^4}} \quad (9)$$

where $\|\cdot\|_F$ denotes the Frobenius norm.

Theorem 5 quantifies asymptotically the relative difference between the DAGAR model and the order free version. Figure 1 plots the quantity on the right hand side of (9) as a function of $\rho \in [0, 1]$. We see that it is a monotonically increasing function of ρ attaining a maximum of $\sqrt{\frac{3}{87}} \approx 0.186$ when $\rho = 1$. Hence, even in the worst case scenario the ordered model differs by less than 20% in terms of Frobenius norm. For small values of ρ the difference is extremely small (0.02 for $\rho = 0.25$) and even for moderate values of ρ (0.5 – 0.75) the difference is around or less than 10%.

Below we also provide the analogous result for the two-dimensional grid graph.

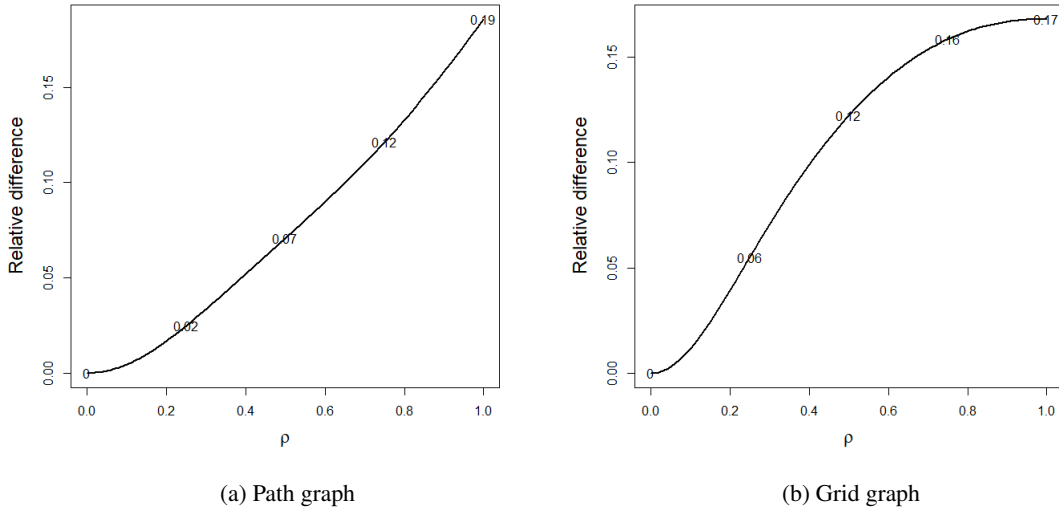


Fig. 1: Asymptotic relative difference between the the DAGAR model and the order free DAGAR model in terms of Frobenius norm for path graph (left) and grid graph (right). The five numbers on each curve corresponds to the values of the difference at $\rho = 0, 0.25, 0.5, 0.75$ and 1 respectively.

THEOREM 6. *Let $Q(\rho)$ be the DAGAR precision matrix for an $m \times m$ grid graph using any of the orderings in Theorem 3. Also let $Q_{OF}(\rho)$ denote the order free DAGAR model. Then*

$$\lim_{m \rightarrow \infty} \frac{\|Q(\rho) - Q_{OF}(\rho)\|_F}{\|Q_{OF}(\rho)\|_F} = \sqrt{\frac{\rho^4 \left(\frac{s(\rho)}{5} - \frac{2}{1+\rho^2} \right)^2 + 2 \left(\frac{1}{3} - \frac{s(\rho)}{30} - \frac{\rho^2}{1+\rho^2} \right)^2 + 12 \left(\frac{1}{6} - \frac{s(\rho)}{60} \right)^2}{(1 + \rho^2 + \rho^2 \frac{s(\rho)}{5})^2 + 4\rho^2 + 20 \left(\frac{1}{6} - \frac{s(\rho)}{60} \right)^2}} \quad (10)$$

where $s(\rho) = \sum_{r=1}^4 \frac{r}{1+(r-1)\rho^2}$.

The limit in Theorem 6 looks more complicated than the analogous result for the path graph. However, things are simplified noting that $1 - s(\rho)/10$ is $O(\rho^2)$ and, hence, so is the numerator in the right hand side of (10). Figure 1 (b) plots this quantity as a function of ρ . We see that once again this is monotonic in ρ and reaches a maximum of around 0.17 when $\rho = 1$. Hence, Q and Q_{OF} differ by at most 17% and the difference is much smaller for lower values of ρ . For both path and grid graphs, the two DAGAR models differ by little for small values of ρ and the worst-case differences were less than 20% for both. While these results are hard to generalise beyond paths and grids to arbitrary graphs, Theorems 5 and 6 provide valuable insight into why the order-free models perform very similar to the DAGAR model for many scenarios.

3. NUMERICAL EXPERIMENTS

3.1. Interpretation of ρ

We conducted numerical experiments to gain insight into the relationship between ρ and the neighbour-pair correlations for the proper conditional autoregressive model, the directed acyclic graph autoregressive model in Section 2.2 and its order-free analogue in Section 2.3. We used

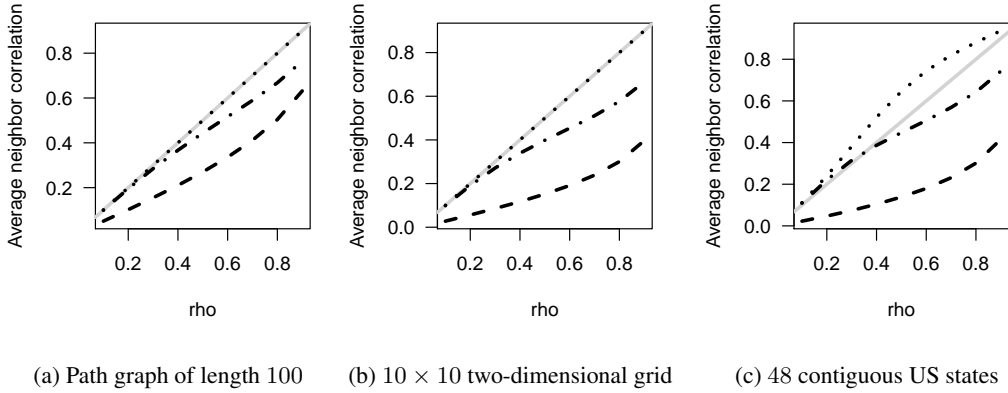


Fig. 2: Average neighbour pair correlations as a function of ρ for proper conditional autoregressive model (dashes), ordered (dots) and order-free (dot-dash) directed acyclic graph autoregressive models. The solid grey line represents $x = y$ line.

three different graphs: a simple path graph with 100 vertices which is analogous to a time-series, a two-dimensional 10×10 lattice or grid graph with edges between vertically or horizontally adjacent vertices, and the state map of contiguous United States, where two states are said to have an edge if they share a common geographical boundary. We generated covariance matrices corresponding to the three models for $\rho \in \{i/10 \mid i = 1, \dots, 9\}$. Figure 2 plots the average neighbour-pair correlation $c(\rho) = \sum_{i \sim j} \text{cov}(w_i, w_j) / (2\sqrt{\text{var}(w_i)}\sqrt{\text{var}(w_j)}) / (\sum n_i)$ as a function of ρ for these three choices of $Q(\rho)$. We see that for the path and grid graph, the average neighbour pair correlation $c(\rho)$ for our ordered model is exactly ρ . This corroborates the results in Theorems 2 and 3. For the highly irregular United States graph, this exact relationship does not hold. Nevertheless, $c(\rho)$ is much closer to ρ than for the proper conditional autoregressive (CAR) model, where even when ρ is close to one, $c(\rho)$ is less than 0.4. In fact, for all three graphs, the average neighbour-pair correlation for the proper conditional autoregressive model remains modest even for very high values of ρ . This has also been observed elsewhere in the literature (Banerjee et al., 2014).

3.2. Simulated data analysis

Models for areal datasets are typically used as priors for areal random effects in a hierarchical setup. For example, let y_i denote the response observed at region i and x_i denote the corresponding set of covariates. A spatial generalised linear mixed model framework assumes $h(E(y_i)) = x_i^T \beta + w_i$ where $h(\cdot)$ denotes a suitable link function. Subsequently, a hierarchical areal model is customarily specified as

$$\prod_{i=1}^k pr(y_i \mid x_i^T \beta + w_i, \theta) \times N(w \mid 0, \tau_w Q(\rho)) \times pr(\beta, \tau_w, \rho, \theta) \quad (11)$$

where $Q(\rho)$ denotes the precision matrix of the areal model, $pr(y_i \mid x_i^T \beta + w_i, \theta)$ denotes the density corresponding to the link $h(\cdot)$ and $pr(\beta, \tau_w, \rho, \theta)$ is the prior for the parameters. If $h(\cdot)$ is the identity link, e.g., the responses are Gaussian, then we can exploit conjugacy for generating w in a sampler. However, for non-Gaussian responses, we have to sample w and the other parameters using a Metropolis random walk sampler from the joint density in (11).

We conducted simulation experiments assessing the performance of the areal data models using the three graph structures described in Section 3.1. For each graph, we embed the vertices on the Euclidean plane and generate the spatial random effect vector w from an exponential Gaussian process, i.e. $w \sim N(0, M/\tau_w)$ where $M = \exp(-\phi d(i, j))$ and $d(i, j)$ denotes the distance between the embedding of the i th and j th vertex, τ_w is the spatial precision and ϕ is the spatial decay. The path graph has a distance preserving embedding in the Euclidean plane such that $D(i, j) = |i - j|$. We embed the grid graph into a 10×10 grid in the Euclidean plane. Although the resulting distance matrix is not identical to the shortest distance (or geodesic) matrix on the graph, the distance between each neighbour-pair remains one. For the United States graph, we use the centroid of each state to create the distance matrix. We scale the distance matrix so that the average neighbour-pair distance is one. To generate w , we use $\tau_w = 0.25$ and $\phi = -\log(j/10)$ for $j = 1, \dots, 9$. This implies that the average neighbour pair correlation $\rho = \exp(-\phi)$ varies between 0.1 and 0.9, thereby covering a wide spectrum of scenarios. Subsequently, we generate the response y comprising independent $y_i = x_i^T \beta + w_i + \epsilon_i$, where x_i is a 2×1 vector comprising two independent standard normal variables, $\beta = (1, 5)^T$, and the ϵ_i 's are independent $N(0, \tau_e)$. Two values of the noise precision τ_e were used so that the ratio $r = \tau_w/\tau_e$ of the spatial and noise precision was 0.1 and 0.5.

We fitted all models using the hierarchical setup in (11) with the four different choices of $Q(\rho)$ — the proper and improper conditional autoregressive models and the ordered and order-free directed acyclic graph autoregressive models. To create the directed acyclic graph for our model, we used the ordering based on the sum of the co-ordinates of the mappings of the vertices. We used conjugate priors $\beta \sim N(0, 1000I)$, $\tau_w \sim \text{Gamma}(2, 1)$ and $\tau_e \sim \text{Gamma}(2, 0.1)$. The spatial correlation parameter ρ was assigned a $\text{Unif}(0, 1)$ prior. For each analysis we used 100,000 Markov chain Monte Carlo iterations with the first 50,000 iterations discarded as burn-in. For each combination of parameter values we used 100 replicate datasets. The posterior estimates of β for all the models were very accurate. This is not surprising as estimates of regression coefficients are typically robust to variance misspecification. However, the posterior estimates of the spatial surfaces were quite different.

Figure 3 plots the mean square error between the true and estimated w averaged over 100 replicates for each scenario. We see that when $r = 0.1$, the mean square errors of the two conditional autoregressive models are higher than the two directed acyclic graph autoregressive models for the most part of all three graphs. The gap is substantially widened when ρ is smaller. In general, for $r = 0.1$ the model in (1) performs the worst among the four. For $r = 0.5$, i.e., when there is more noise, our models tend to produce better mean square errors for values of ρ less than approximately 0.5. However, the trend reverses for larger values of ρ , where (1) seems to outperform the other three models. Hence, only when there is substantial noise and strong spatial correlation among the random effects, using the improper conditional autoregressive model is beneficial and outperforms the other three models. For all other scenarios our models produce considerably lower mean square errors. We also noticed that there was very little difference between the performance of our model (7) and its order-free analogue (8) for most of the scenarios. This result is encouraging as the scalability of the former implies it offers a pragmatic solution for analysing very large areal datasets or networks.

4. SLOVENIA STOMACH CANCER DATA

In this Section we analyse a dataset on stomach cancer rates in Slovenia. The dataset consists of observed (O_i) and expected (E_i) number of cancer counts for each of the 194 municipalities of the country. Previous studies have analysed this dataset to understand the relationship between

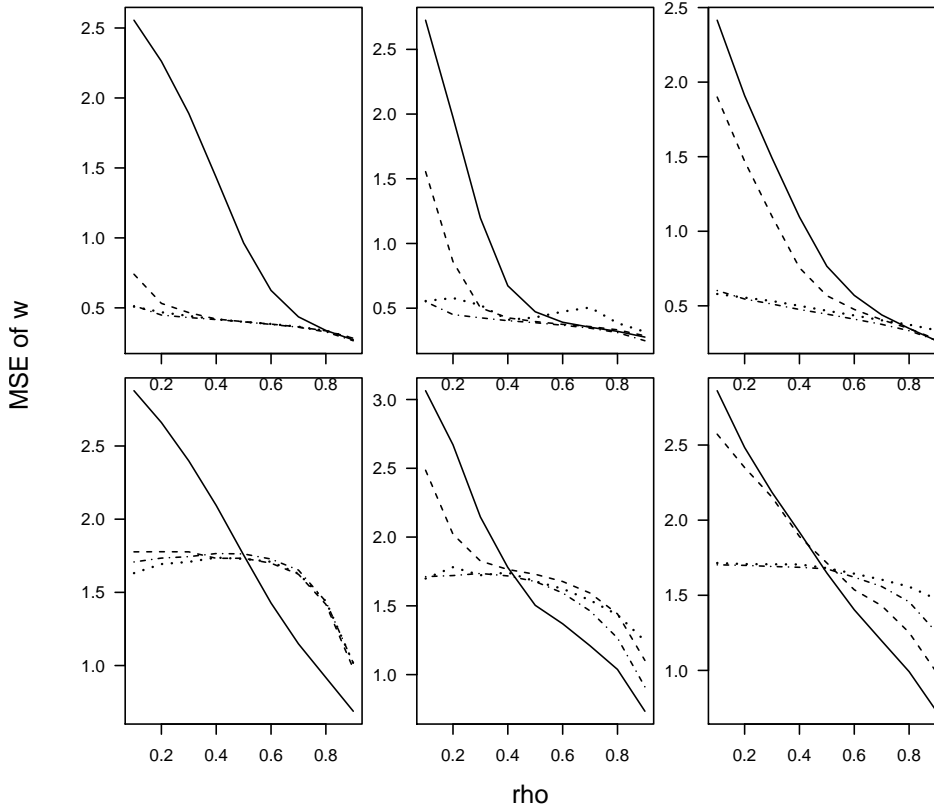


Fig. 3: Mean Square Error between true and estimated w for for improper (solid) and proper (dashes) conditional autoregressive models and ordered (dots) and order-free (dot-dash) directed acyclic graph autoregressive models. Top and bottom row correspond to $r = 0.1$ and 0.5 respectively. Left, middle and right columns correspond to path, grid and United States graphs.

cancer incidence rates and socioeconomic factors (Reich et al., 2006; Zadnik & Reich, 2006). The covariate representing socio-economic status was defined for each county by Slovenia's Institute of Macroeconomic Analysis and Development and is an ordinal variable (SE_i) taking values in $1, \dots, 5$. We analysed this dataset using Poisson spatial regression model where each O_i is modelled as an independent Poisson random variable with mean $E_i \exp(\alpha + \beta SE_i + w_i)$ where $w \sim N(0, \tau_w Q(\rho))$. We assign α and β independent nearly flat $N(0, 10000)$ priors. The three models for $Q(\rho)$ in 3.1 and the same Markov chain Monte Carlo specifications as in Section 3.2 were used. In addition to presenting the parameter estimates, we also used model comparison to assess the three covariance models. We used the Deviance Information Criterion (Spiegelhalter et al., 2002) to compare the posterior distributions. Since the dataset under investigation here is moderately small with 194 regions, we also conducted a leave-one-out analysis and estimated the leave-one-out cross validated log posterior predictive density.

We summarise the results in Table 1. For all three models the confidence intervals for α and β lie outside zero and the estimated coefficient of β is negative. Contrasting these estimates with those obtained in Zadnik & Reich (2006) we note that unlike the improper CAR model, where spatial confounding debilitated the negative association of cancer rates with socio-economic sta-

Table 1: Parameter estimates (posterior medians) and model comparison metrics for the Slovenia data analysis. The numbers inside braces indicates the lower and upper bounds for the 95% credible intervals

	α	β	ρ	DIC	LPPD _{CV}
CAR	0.09 (0.02, 0.16)	-0.12 (-0.19, -0.04)	0.33 (0.02, 0.86)	1097	1170
DAGAR	0.11 (0.03, 0.18)	-0.12 (-0.19, -0.06)	0.08 (0.004, 0.24)	1091	1127
DAGAR _{OF}	0.11 (0.05, 0.17)	-0.12 (-0.18, -0.06)	0.06 (0.003, 0.2)	1090	1133

CAR, Proper conditional autoregressive model; DAGAR, Directed acyclic graph autoregressive model; DAGAR_{OF}, Order-free DAGAR model; DIC: Deviance Information Criterion; LPPD_{CV}: Cross-validated log posterior predictive density.

tus ($\hat{\beta}_{ICAR} = -0.02 (-0.10, 0.06)$), all three model estimates here retained this association. In fact the estimates of β here were closer to those obtained in the non-spatial (NS) analysis ($\hat{\beta}_{NS} = -0.14 (-0.17, -0.10)$). Perhaps this is an artefact of the relatively small estimate of ρ obtained from all three models indicating a weak spatial correlation (unlike the improper conditional autoregressive model which assumes $\rho = 1$). This once again demonstrates the value of the added flexibility of the parametrised models. Among the three models used here, the confidence interval of ρ was much tighter for our models than the proper conditional autoregressive model where ρ had little posterior learning. The DIC estimates for the three models were extremely close with our models being marginally better. The cross-validated log-posterior predictive density estimates showed a more substantial difference with our proposed models once again performing better. The results for the order-dependent model (7) and the order-free model (8) were once again very close both in terms of parameter estimates and model comparisons.

5. DISCUSSION

No single model is guaranteed to provide the best fit for every areal dataset and it is desirable to have different models tailored to different types of features in the data. The existing repertoire of covariance models used for analysing areal datasets is extremely limited. In this manuscript, we have developed an alternative parametric model for areal datasets that promises to be a significant addition to this inventory. The parametric DAGAR models we have proposed in Section 2 are novel and do not correspond to any intrinsic autoregressive model or the proper CAR model. DAGAR model offers greater degree of interpretability and flexibility, and will be scalable for large datasets. We observe that for a large number of scenarios the DAGAR model performs better than both variants of the CAR model and believe this will be a useful alternative to the CAR models for analysing many aerial disease mapping datasets.

For most of our data analyses, we observed that the ordered model yields results almost indistinguishable from the order-free version. The FLOPs count and memory requirement for the ordered model is exactly linear in the size of the dataset k . The precision matrix for the order-free model, although sparse, can entail expensive determinant calculations. The FLOPs count for the proper conditional autoregressive model is also linear in k . However, this scalability is contingent upon an expensive eigen-value decomposition which requires $\mathcal{O}(k^2)$ storage and one time usage of up to $\mathcal{O}(k^3)$ flops (Jin et al., 2005). Furthermore, variants of this model that do not assume a known adjacency matrix (Lu et al., 2007) or the one proposed in Leroux et al. (2000) do not enjoy this linear scalability. For large datasets the ordered model (7) will remain scalable while the other models may run several orders of magnitude slower. Hence, if expediency is the prior-

ity, we recommend using the ordered model. While the dependence on the ordering may appear uncomfortable, Theorems 5 and 6 provide some insights into why the ordered model performs similar to the order-free one and substantive inference is expected to be robust to the ordering.

Analysing prevalence of many diseases simultaneously in a multivariate setup is becoming increasingly important to accommodate the correlations among different disease prevalences. Many of the popular approaches rely on Cholesky factors of conditionally autoregressive precision matrices (Gelfand & Vounatsou, 2003; Martinez-Beneito, 2013; Martinez-Beneito et al., 2017) which can be computationally prohibitive for large k . Our ordered model lends itself naturally to these settings due to the readily available Cholesky decomposition and, hence, promises to broaden the inventory of multivariate disease mapping models. The ordered model also offers a coherent way of modelling on arbitrary graphs or networks of growing size, i.e., if a new point is added to the graph, the nested distributions remain same, unlike any of the other three models considered here.

A. PROOFS

A.1. Theorem 1

Let $r = \text{rank}(Q)$ and Q^+ denote the Moore-Penrose inverse of Q . Then, by Theorem 1 part (b) of Higham (1990), there exists a permutation P such that

$$PQ^+P^\top = R^\top R \text{ where } R = \begin{bmatrix} R_1 & R_2 \\ 0 & 0 \end{bmatrix}$$

Here R_1 is $r \times r$ upper triangular matrix with positive diagonal elements. Let $D_1 = \text{diag}(R_1)$ and $R_1^* = D_1^{-1}R_1$, which has ones on the diagonal. We can now write

$$R = DU \text{ where } U = \begin{bmatrix} R_1^* & D_1^{-1}R_2 \\ 0 & I \end{bmatrix} \text{ and } D = \begin{bmatrix} D_1 & 0 \\ 0 & 0 \end{bmatrix}$$

Since U^\top is a lower triangular matrix with one on the diagonals, so is $L = U^{-\top}$. Hence, $PQP^\top = (I - B)^\top F(I - B)$ where $F = D^{+2}$ and $B = I - L$ is a strictly lower triangular matrix.

A.2. Theorem 2

First of all, as \mathcal{T} is a tree, it is always possible to have an ordering π such that $n_\pi(i) = 1$ for any $i \neq \pi(1)$. For example, the orderings corresponding to any pre-order or breadth-first tree traversal of \mathcal{T} will satisfy this. Without loss of generality we rename the nodes such that $\pi = \{1, \dots, k\}$ and for $i > 1$, $p(i)$ denotes the directed neighbour of i in π implying $p(i) < i$. Letting $w_0 = 0$, $p(1) = 0$ and $n_\pi(1) = 0$, the model in (6) reduces to $w_i = \rho w_{p(i)} + (1 - \rho^2)^{0.5} \epsilon_i$ where ϵ_i are independent standard normal variables. We shall show that for any positive integers $j \leq i \leq k$, $\text{cov}(w_i, w_j) = \rho^{d_{ij}}$. We prove this using the strong form of mathematical induction. Since $p(2) = 1$, it is easy to verify this for $i = 2$. We assume that this is true for $i = 2, \dots, i - 1$. It immediately follows that $\text{var}(w_i) = \rho^2 \text{var}(w_{p(i)}) + (1 - \rho^2) \text{var}(\epsilon_i) = 1$. For any $j < i$, $\text{cov}(w_i, w_j) = \rho \text{cov}(w_{p(i)}, w_j) = \rho^{1+d_{p(i)j}}$ (by induction). Since \mathcal{T} is acyclic and $n_\pi(i) = 1$ for all $i > 1$, the shortest path from j to i runs through $p(i)$. Hence, $d_{ij} = d_{p(i)j} + 1$ and the result follows.

A.3. Theorem 3

If $i + j = i' + j'$, then (i, j) and (i', j') are never neighbours. Hence, without loss of generality, we prove the result for $\pi = (S_2, \dots, S_{m+n})^\top$ where $S_r = \{(i, j) \mid i + j = r\}$. Let $d((i, j), (i', j')) = |i - i'| + |j - j'|$ denote the Manhattan distance on \mathcal{G} , and w_{S_r} denote the subvector of w corresponding to the indices in S_r . We first show by induction on r that $w_{S_r} \sim N(0, (\rho^{D_r})^{-1})$ where D_r denotes the distance matrix on S_r . It is easy to see that this holds for $r = 2$. Let us assume that it holds true for $r - 1$. If $(1, r - 1) \in S_r$, we define $w(0, r - 1) = \rho w(1, r - 1) + \epsilon(0, r - 1)$ where $\epsilon(0, r - 1) \sim$

$N(0, 1/(1 - \rho^2))$ is independent of w . If $(r - 1, 1) \in S_r$ we define $w(r - 1, 0)$ similarly. Let $w_{S_{r-1}}^*$ be the augmented vector which includes $w(0, r - 1)$ or $w(r - 1, 0)$ or both, along with $w_{S_{r-1}}$. From the construction, $w(0, r - 1) = \rho^2 w(1, r - 2) + \rho \epsilon(1, r - 1) + \epsilon(0, r - 1)$ implying $\text{var}(w(0, r - 1)) = 1$ and $\text{cov}(w(0, r - 1), w(1, r - 2)) = \rho^2$. Hence $\text{cov}(w_{S_{r-1}}^*) = \rho^{D_r^*}$ where D_r^* is the augmented distance matrix corresponding to S_{r-1} . Letting $\rho^2 = u$, we have for any (i, j) and (i', j') in S_r ,

$$\begin{aligned} \text{cov}(w(i, j), w(i', j')) &= \frac{u}{(1+u)^2} (\text{cov}(w(i-1, j), w(i'-1, j')) + \text{cov}(w(i, j-1), w(i'-1, j'))) \\ &\quad + \text{cov}(w(i-1, j), w(i', j'-1)) + \text{cov}(w(i, j-1), w(i', j'-1))) + I(i = i') \frac{1-u}{1+u} \\ &= \frac{u}{(1+u)^2} (\rho^{|i-i'+1|+|j-j'-1|} + 2\rho^{|i-i'|+|j-j'|} + \rho^{|i-i'-1|+|j-j'+1|}) + I(i = i') \frac{1-u}{1+u} \end{aligned}$$

If $i = i'$ then $j = j'$ and the expression above equals 1. If $i < i'$, then $j > j'$ and $|i - i' + 1| + |j - j' - 1| = (i' - i - 1) + (j - j' - 1) = |i - i'| + |j - j'| - 2$. Similarly, $|i - i' - 1| + |j - j' + 1| = |i - i'| + |j - j'| + 2$. So, $\rho^{|i-i'+1|+|j-j'-1|} + 2\rho^{|i-i'|+|j-j'|} + \rho^{|i-i'-1|+|j-j'+1|} = \rho^{|i-i'|+|j-j'|} (1/u + 2 + u)$. Hence, the results follows.

A.4. Theorem 4

For any vertex i with n_i neighbours, let Π_{ir} denote the set of all permutations π such that $n_{\pi(i)} = r$. By symmetry, $|\Pi_{ir}| = k!/(n_i + 1)$ for $r = 0, 1, \dots, n_i$. Also, for any $i \sim j$ and $r = 0, \dots, n_i$, let Π_{ijr} denote the set of all permutations π such that $n_{\pi(i)} = r$ and $j \in N_{\pi}(i)$. Then, $|\Pi_{ijr}| = k!/(n_i + 1) \times pr(j)$ among the r directed neighbours of i is $rk!/(n_i(n_i + 1))$. We now have

$$\begin{aligned} Q[i, i] &= \frac{1}{k!(1 - \rho^2)} \sum_{\pi} \left(1 + (n_{\pi(i)} - 1)\rho^2 + \sum_{j \sim i} I(i \in N_{\pi}(j)) \frac{\rho^2}{1 + (n_{\pi(j)} - 1)\rho^2} \right) \\ &= 1 + \frac{\rho^2}{k!(1 - \rho^2)} \left(\sum_{r=0}^{n_i} r |\Pi_r| + \sum_{j \sim i} \sum_{r=0}^{n_j} \frac{|\Pi_{jir}|}{1 + (r - 1)\rho^2} \right) \\ &= 1 + \frac{n_i \rho^2}{2(1 - \rho^2)} + \frac{\rho^2}{1 - \rho^2} \sum_{j \sim i} \frac{1}{n_j(n_j + 1)} \sum_{r=1}^{n_j} \frac{r}{1 + (r - 1)\rho^2} \\ &= 1 + \frac{n_i \rho^2}{2(1 - \rho^2)} + \frac{\rho^2}{1 - \rho^2} \sum_{j \sim i} \frac{1}{n_j(n_j + 1)} f(\rho, n_j). \end{aligned}$$

To evaluate the non-diagonal entries of Q , we additionally define Π_{ijk_r} to be the set of all permutations π such that $n_{\pi(i)} = r$ and $\{j, k\} \subseteq N_{\pi}(i)$. Applying the combinatorial argument used earlier, we see that $|\Pi_{ijk_r}| = r(r - 1)k! / ((n_i - 1)n_i(n_i + 1))$. Let $i \approx j$ implies that there exists at least one node k such that $i \sim k$ and $j \sim k$.

$$\begin{aligned} Q[i, j] &= \frac{1}{k!(1 - \rho^2)} \sum_{\pi} \left(-\rho I(i \sim j) + I(i \approx j) \sum_{k: \{i, j\} \subseteq N_{\pi}(k)} \frac{\rho^2}{1 + (n_{\pi(k)} - 1)\rho^2} \right) \\ &= -\frac{\rho}{1 - \rho^2} I(i \sim j) + \frac{\rho^2}{k!(1 - \rho^2)} I(i \approx j) \sum_{k \sim N(i) \cap N(j)} \sum_{r=0}^{n_k} \frac{|\Pi_{kij_r}|}{1 + (r - 1)\rho^2} \\ &= -\frac{\rho}{1 - \rho^2} I(i \sim j) + \frac{\rho^2}{1 - \rho^2} I(i \approx j) \sum_{k \sim N(i) \cap N(j)} \frac{1}{(n_k - 1)n_k(n_k + 1)} \sum_{r=1}^{n_k} \frac{r(r - 1)}{1 + (r - 1)\rho^2} \\ &= -\frac{\rho}{1 - \rho^2} I(i \sim j) + \frac{1}{1 - \rho^2} I(i \approx j) \sum_{k \sim N(i) \cap N(j)} \left(\frac{1}{2(n_k - 1)} - \frac{1}{(n_k - 1)n_k(n_k + 1)} f(\rho, n_k) \right). \end{aligned}$$

A.5. *Theorem 5*

We write $Q(\rho)$ and $Q_{OF}(\rho)$ as Q and Q_{OF} hiding the dependence on ρ except when necessary. From Theorem 4 we have for $i = 3, \dots, k-2$, $Q_{OF:ii} = \frac{3+6\rho^2+\rho^4}{3(1+\rho^2)(1-\rho^2)}$, $Q_{OF:i,i+1} = -\frac{\rho}{1-\rho^2}$ and $Q_{OF:i,i+2} = \frac{\rho^2}{3(1+\rho^2)(1-\rho^2)}$. Hence,

$$\|Q_{OF}\|_F^2 = \frac{k}{9(1+\rho^2)^2(1-\rho^2)^2} ((3+6\rho^2+\rho^4)^2 + 18\rho^2(1+\rho^2)^2 + 2\rho^4) + o(k)$$

where the $o(k)$ term arises from rows and columns corresponding to the nodes at the extreme right or left.

Now using left-to-right or right-to-left ordering, from (5), a typical term in the quadratic form $w'Qw$ will be of the form $(w_i - \rho w_{i-1})^2/(1-\rho^2)$. Hence, for $i = 1, 2, \dots, k-2$, $Q_{ii} = \frac{1+\rho^2}{1-\rho^2}$, $Q_{i,i+1} = -\frac{\rho}{1-\rho^2}$ and $Q_{i,i+2} = 0$. So,

$$\begin{aligned} \|Q_{OF} - Q\|_F^2 &= \frac{k}{9(1+\rho^2)^2(1-\rho^2)^2} ((3+6\rho^2+\rho^4 - 3(1+\rho^2)^2)^2 + 2\rho^4) + o(k) \\ &= \frac{k}{9(1+\rho^2)^2(1-\rho^2)^2} (4\rho^8 + 2\rho^4) + o(k) \end{aligned}$$

Hence, the result follows.

A.6. *Theorem 6*

We index the nodes of the grid as (i, j) , and entries of Q and Q_{OF} as $Q_{(ij),(i'j')}$ and $Q_{OF:(ij),(i'j')}$ respectively for $1 \leq i, i', j, j' \leq m$. Like in the proof of Theorem 5, it only suffices to evaluate the Frobenius norms for the interior points of the grid (having 4 neighbors each of whom also have 4 neighbors) as the contribution from the remaining grid terms will be $o(m^2)$. Hence from Theorem 3 we have for $3 \leq i, i', j, j' \leq m-2$,

$$\begin{aligned} Q_{OF:(ij),(ij)} &= \frac{1+\rho^2+\rho^2s(\rho)/5}{1-\rho^2} \\ Q_{OF:(ij),(i+1,j)} &= Q_{OF:(ij),(i,j+1)} = -\frac{\rho}{1-\rho^2} \\ Q_{OF:(ij),(i+2,j)} &= Q_{OF:(ij),(i,j+2)} = \frac{1}{1-\rho^2}(1/6 - s(\rho)/60) \\ Q_{OF:(ij),(i+1,j+1)} &= Q_{OF:(ij),(i+1,j-1)} = \frac{2}{1-\rho^2}(1/6 - s(\rho)/60) \end{aligned}$$

Summing up, we have

$$\begin{aligned} \|Q_{OF}\|_F^2 &= m^2(Q_{OF:(ij),(ij)}^2 + 4(Q_{OF:(ij),(i+1,j)}^2 + Q_{OF:(ij),(i+2,j)}^2 + Q_{OF:(ij),(i+1,j+1)}^2) + o(1)) \\ &= \frac{m^2}{(1-\rho^2)^2} ((1+\rho^2+\rho^2s(\rho)/5)^2 + 4\rho^2 + 20(1/6 - s(\rho)/60)^2) + o(m^2) \end{aligned}$$

Now, without loss of generality we assume that the DAGAR precision matrix $Q(\rho)$ was constructed by ordering the nodes in increasing order of $(i+j)$. Then, using (5), a typical term in the quadratic form $w'Qw$ will be of the form $\frac{1+\rho^2}{1-\rho^2}(w_{ij} - \frac{\rho}{1+\rho^2}(w_{i,j-1} + w_{i-1,j}))^2$. Hence, we will have

$$\begin{aligned} Q_{(ij),(ij)} &= \frac{1+\rho^2+2\rho^2/(1+\rho^2)}{1-\rho^2} \\ Q_{(ij),(i+1,j)} &= Q_{(ij),(i,j+1)} = -\frac{\rho}{1-\rho^2} \\ Q_{(ij),(i+2,j)} &= Q_{(ij),(i,j+2)} = Q_{(ij),(i+1,j+1)} = 0 \\ Q_{(ij),(i+1,j-1)} &= \frac{\rho^2}{(1+\rho^2)(1-\rho^2)} \end{aligned}$$

Subtracting, we have

$$\begin{aligned} \|Q - Q_{OF}\|_F^2 = & m^2((Q_{(ij),(ij)} - Q_{OF:(ij),(ij)})^2 + 4Q_{OF:(ij),(i+2,j)}^2 + \\ & 2(Q_{(ij),(i+1,j-1)} - Q_{OF:(ij),(i+1,j-1)})^2 + \\ & 2Q_{OF:(ij),(i+1,j+1)}^2 + o(1)) \end{aligned}$$

Hence, the result follows.

REFERENCES

- ASSUNCAO, R. & KRAINSKI, E. (2009). Neighborhood dependence in Bayesian spatial models. *Biometrical Journal* **51**, 851–869.
- BANERJEE, S., CARLIN, B. P. & GELFAND, A. E. (2014). *Hierarchical Modeling and Analysis for Spatial Data*. Boca Raton, FL: Chapman & Hall/CRC, 2nd ed.
- BASSEVILLE, M., BENVENISTE, A., CHOU, K. C., GOLDEN, S. A., NIKOUKHAH, R. & WILLSKY, A. S. (2006). Modeling and estimation of multiresolution stochastic processes. *IEEE Trans. Inf. Theor.* **38**, 766–784.
- BESAG, J. (1974). Spatial interaction and statistical analysis of lattice systems. *Journal of the Royal Statistical Society, Series B* **36**, 192–225.
- BESAG, J. & HIGDON, D. (1999). Bayesian analysis of agricultural field experiments. *Journal of the Royal Statistical Society: Series B (Statistical Methodology)* **61**, 691–746.
- BESAG, J. & KOOPERBERG, C. (1995). On conditional and intrinsic autoregressions. *Biometrika* **82**, 733–746.
- BESAG, J. & MONDAL, D. (2005). First-order intrinsic autoregressions and the de wijs process. *Biometrika* **92**, 909–920.
- BICKEL, P. J. & LEVINA, E. (2008a). Covariance regularization by thresholding. *The Annals of Statistics* **36**, 2577–2604.
- BICKEL, P. J. & LEVINA, E. (2008b). Regularized estimation of large covariance matrices. *The Annals of Statistics* **36**, 199–227.
- CAI, T. T., ZHANG, C.-H. & ZHOU, H. H. (2010). Optimal rates of convergence for covariance matrix estimation. *The Annals of Statistics* **38**, 2118–2144.
- CLAYTON, D. G. & BERNARDINELLI, L. (1992). Bayesian methods for mapping disease risk. In *Geographical and Environmental Epidemiology: Methods for Small-Area Studies*, P. Elliott, J. Cuzick, D. English & R. Stern, eds. Oxford University Press, pp. 205–220.
- CRESSIE, N. & DAVIDSON, J. L. (1998). Image analysis with partially ordered Markov models. *Computational Statistics and Data Analysis* **29**, 1–26.
- DATTA, A., BANERJEE, S., FINLEY, A. O. & GELFAND, A. E. (2016a). Hierarchical nearest-neighbor Gaussian process models for large geostatistical datasets. *Journal of the American Statistical Association* **111**, 800–812.
- DATTA, A., BANERJEE, S., FINLEY, A. O., HAMM, N. A. S. & SCHAAP, M. (2016b). Nonseparable dynamic nearest neighbor Gaussian process models for large spatio-temporal data with an application to particulate matter analysis. *Ann. Appl. Statist.* **10**, 1286–1316.
- DUTTA, S. & MONDAL, D. (2015). An h-likelihood method for spatial mixed linear models based on intrinsic auto-regressions. *Journal of the Royal Statistical Society: Series B (Statistical Methodology)* **77**, 699–726.
- EL KAROUI, N. (2008). Operator norm consistent estimation of large-dimensional sparse covariance matrices. *The Annals of Statistics* **36**, 2717–2756.
- FINLEY, A. O., DATTA, A., COOK, B. C., MORTON, D. C., ANDERSEN, H. E. & BANERJEE, S. (2017). Applying nearest neighbor Gaussian processes to massive spatial data sets: Forest canopy height prediction across Tanana Valley Alaska. <https://arxiv.org/pdf/1702.00434.pdf>.
- FRIEDMAN, J., HASTIE, T. & TIBSHIRANI, R. (2007). Sparse inverse covariance estimation with the graphical lasso. *Biostatistics* **9**, 432–441.
- GELFAND, A. E. & VOUNATSOU, P. (2003). Proper multivariate conditional autoregressive models for spatial data analysis. *Biostatistics* **4**, 11.
- HIGHAM, N. J. (1990). Analysis of the cholesky decomposition of a semi-definite matrix. In *in Reliable Numerical Computation*. University Press.
- HINTON, G. E. (2002). Training products of experts by minimizing contrastive divergence. *Neural Computation* **14**, 1711–1800.
- HOETING, J. A., MADIGAN, D., RAFTERY, A. E. & VOLINSKY, C. T. (1999). Bayesian model averaging: a tutorial (with comments by M. Clyde, David Draper and E. I. George, and a rejoinder by the authors. *Statist. Sci.* **14**, 382–417.
- JIN, X., CARLIN, B. & BANERJEE, S. (2005). Generalized hierarchical multivariate CAR models for areal data. *Biometrics* **61**, 950–961.

- LEROUX, B. G., LEI, X. & BRESLOW, N. (2000). Estimation of disease rates in small areas: A new mixed model for spatial dependence. In *Statistical Models in Epidemiology, the Environment, and Clinical Trials*, M. E. Halloran & D. Berry, eds. New York, NY: Springer New York, pp. 179–191.
- LU, H., REILLY, C. S., BANERJEE, S. & CARLIN, B. P. (2007). Bayesian areal wombling via adjacency modeling. *Environmental and Ecological Statistics* **14**, 433–452.
- MACNAB, Y. & DEAN, C. (2000). Parametric bootstrap and penalized quasi-likelihood inference in conditional autoregressive models. *Statistics in Medicine* **19**, 15–30.
- MARTINEZ-BENEITO, M. A. (2013). A general modelling framework for multivariate disease mapping. *Biometrika* **100**, 539.
- MARTINEZ-BENEITO, M. A., BOTELLA-ROCAMORA, P. & BANERJEE, S. (2017). Towards a multidimensional approach to Bayesian disease mapping. *Bayesian Anal.* **12**, 239–259.
- MEINSHAUSEN, N. & BUHLMANN, P. (2006). High-dimensional graphs and variable selection with the lasso. *The Annals of Statistics* **34**, 1436–1462.
- REICH, B. J., HODGES, J. S. & ZADNIK, V. (2006). Effects of residual smoothing on the posterior of the fixed effects in disease-mapping models. *Biometrics* **62**, 1197–1206.
- ROTHMAN, A. J., LEVINA, E. & ZHU, J. (2009). Generalized thresholding of large covariance matrices. *Journal of the American Statistical Association* **104**, 177–186.
- SPIEGELHALTER, D. J., BEST, N. G., CARLIN, B. P. & VAN DER LINDE, A. (2002). Bayesian measures of model complexity and fit. *Journal of the Royal Statistical Society, Series B* **64**, 583–639.
- STEIN, M. L. (1999). *Interpolation of Spatial Data: Some Theory for Kriging*. New York, NY: Springer, 1st ed.
- STEIN, M. L., CHI, Z. & WELTY, L. J. (2004). Approximating likelihoods for large spatial data sets. *Journal of the Royal Statistical Society, Series B* **66**, 275–296.
- SUDDERTH, E. B. (2002). Embedded trees: Estimation of Gaussian processes on graphs with cycles. <http://cs.brown.edu/sudderth/papers/sudderthMasters.pdf>.
- VECCHIA, A. V. (1988). Estimation and model identification for continuous spatial processes. *Journal of the Royal Statistical Society, Series B* **50**, 297–312.
- WALL, M. (2004). A close look at the spatial structure implied by the CAR and SAR models. *Journal of Statistical Planning and Inference* **121**, 311–324.
- WHITTLE, P. (1954). On stationary processes in the plane. *Biometrika* **41**, 434–449.
- WU, W. & POURAHMADI, M. (2003). Nonparametric estimation of large covariance matrices of longitudinal data. *Biometrika* **90**, 831–844.
- XUE, L., MA, S. & ZOU, H. (2012). Positive-definite ℓ_1 -penalized estimation of large covariance matrices. *Journal of the American Statistical Association* **107**, 1480–1491.
- ZADNIK, V. & REICH, B. J. (2006). Analysis of the relationship between socioeconomic factors and stomach cancer incidence in Slovenia. *Neoplasma* **53**, 103–110.